

1 **The utility of height for the Ediacaran organisms of Mistaken Point**

2
3 **Authors:** Emily. G. Mitchell*¹, Charlotte. G. Kenchington^{1,2}.

4 **Affiliations:**

5 ¹ Department of Earth Sciences, University of Cambridge, Downing Street, Cambridge, CB2
6 3EQ, UK.

7 ²Department of Earth Sciences, Memorial University of Newfoundland, 230 Elizabeth Ave, St.
8 John's, NL A1B 3X9, Canada.

9 *Correspondence to: ek338@cam.ac.uk. Phone: +44 1223 333 416

10

11 **Ediacaran fossil communities consist of the oldest macroscopic eukaryotic organisms.**
12 **Increased size (height) is hypothesized to be driven by competition for water-column**
13 **resources, leading to vertical/epifaunal tiering and morphological innovations such as**
14 **stems. Using spatial analyses, we find no correlation between tiering and resource**
15 **competition, and that stemmed organisms are not tiered. Instead, we find height is**
16 **correlated to greater offspring dispersal, demonstrating the importance of colonization**
17 **potential over resource competition.**

18 Bedding-plane assemblages of Ediacaran fossils at Mistaken Point, Newfoundland (~566
19 Ma)¹, are among the oldest known eukaryotic microfossil communities². In extant marine
20 ecosystems, body size is key to structuring communities, due to size-structured predation
21 dynamics^{3,4}. However, the Mistaken Point communities pre-date macro-predation and
22 (extensive) mobility⁵, and so body size must have played a different role. Instead, the driver of
23 large size has been suggested to be competition for vertically distributed water-column
24 resources, resulting in different taxa occupying different parts of the water column – a process
25 known as tiering⁶. Consequently, tiering to avoid resource competition has been interpreted as
26 the major driver in the diversification of Ediacaran body plans, most notably in the evolution of a
27 non-branched (i.e. “naked”) stem⁷⁻⁹. Since Mistaken Point bedding planes consist of sessile
28 organisms preserved *in-situ*, it is reasonable to assume that approximately all of the macroscopic
29 organisms were preserved, so the bedding planes represent a near-census of the community at the
30 time of burial². Therefore, detailed statistical analyses of these populations and their spatial
31 distributions can be used to determine the relationship between height and resource
32 competition^{10,11}.

33 We analysed the communities of three large bedding-plane assemblages in the Mistaken
34 Point Ecological Reserve: the ‘D’, ‘E’, and Lower Mistaken Point (LMP) surfaces¹², using the
35 data from [11] (Supplementary Figure 1). These communities are dominated by rangeomorphs,
36 a clade of “fractally-branching” organisms^{13,14,15} with some taxa also possessing a naked stem⁷.
37 These communities also include non-fractally branching frondose arboreomorphs¹⁶; the putative
38 sponge *Thectardis*; fronds awaiting formal description (e.g. “Ostrich Feathers”)²; and irregular
39 bedding-plane features referred to as ivesheadiomorphs and “Lobate Discs”^{2,10,17} (see Methods
40 for details). Community composition differs between the three communities, with the ‘D’ surface
41 notably different due to exclusive population by rangeomorphs with no abundant stemmed taxa
42 (Supplementary Table 2). All three assemblages occur within deep-marine turbidite sequences²,
43 with fossils preserved as external moulds in siltstone hemipelagites, cast from above by
44 volcanoclastic deposits¹⁸ (Supplementary Figure 1). A volcanic tuff directly above the ‘E’ surface
45 has been dated to 566.25±0.35Ma, which provides an upper age constraint on the underlying ‘D’
46 and LMP surfaces¹⁹.

47 To quantify the extent of tiering, we calculated the percentage by which each taxon’s
48 population exhibits distinct vertical stratification (*DVS*) with respect to the rest of the community
49 (Supplementary Figure 2). The extent of community tiering is defined as the mean taxa *DVS*.
50 Two different *DVS* metrics were calculated: height-based *DVS*^{height} and uptake-zone *DVS*^{uptake}.
51 The taxon-specific *DVS*^{height} is defined as the percentage of specimens within the taxon
52 population that are not matched in height by any specimen from a different taxonomic group
53 (Supplementary Figure 2). Taxon-specific *DVS*^{uptake} is defined as the percentage of specimens
54 within a taxon population whose “uptake-zone” (i.e. the branching organism part) is not in the
55 same part of the water column as the uptake-zone of specimens from a different taxonomic group

56 (Supplementary Figure 2 and Methods). Consequently, $DVS=0\%$ corresponds to no tiering while
57 $DVS=100\%$ corresponds to a completed tiered community.

58 Competition was detected and quantified using spatial point process analyses, whereby
59 pair correlation functions (PCFs) were calculated to describe the spatial distributions between
60 pairs of taxa on each bedding plane²⁰, with a $PCF=1$ indicating a distribution that was
61 completely spatially random (CSR), $PCF>1$ indicating aggregation, and $PCF<1$ indicating
62 segregation²⁰⁻²². Monte Carlo simulations and Diggle's goodness-of-fit test²² (p_d) were used to
63 indicate significantly non-CSR distributions when the observed PCF deviated outside the
64 simulation envelope coupled with a $p_d \ll 1$. Where bivariate spatial segregation was detected,
65 partial PCF between size-classes (defined in Methods; Supplementary Figure 3) were calculated,
66 and Diggle's segregation test²³ used to assess segregation of each size class. Identifying the
67 processes behind spatial patterns is not straightforward²²⁻²⁷; however, inter-specific resource
68 competition typically generates a segregated pattern, with segregated largest specimens and CSR
69 or aggregated small specimens²¹. To further investigate the relationship of height with dispersal
70 dynamics, the mean cluster radius was calculated by fitting univariate Thomas cluster models to
71 the univariate PCFs²⁷ (Supplementary Table 4). Linear regressions of these radii were then fitted
72 to mean height, maximum height and mean uptake-zone height for each frondose taxon
73 (Supplementary Table 5).

74 Only the 'D' surface was found to exhibit high DVS (80.1% , Figure 1, Supplementary
75 Table 1. $DVS^{height}_D = DVS^{uptake}_D$). In contrast, the DVS^{height} for the 'E' surface community is only
76 12.4%, and only 20.0% for the LMP community (Supplementary Table 1), DVS^{uptake} was larger
77 than DVS^{height} ($DVS^{uptake}_E = 44.9\%$; $DVS^{uptake}_{LMP} = 40.9\%$), but still under 50%. Taxon DVS^{height}
78 and DVS^{uptake} are not significantly different between the LMP, 'D' or 'E' communities ($p=0.10$

79 and $p=0.37$) or DVS^{height} between ‘D’ and ‘E’ communities ($p=0.03$; $\alpha=0.016$). There are no
80 instances of large spatial-scale bivariate segregation on the ‘D’ surface and two on the ‘E’
81 surface (cf. [10]); Figure 2 and Supplementary Table 3). On the ‘E’ surface, spatial segregation
82 is found between *Fractofusus* and Feather Dusters ($PCF_{Min}=0.8852$; $p=0.01$), and between
83 Feather Dusters and *Charniodiscus* ($PCF_{Min}=0.8972$; $p=0.01$) with segregation detected between
84 large specimens (both $p=0.01$), but not between small specimens ($p_{feaD-Fract}=0.25$ and p_{feaD-}
85 $Chard=0.14$; Supplementary Table 3, Figure 2a,b). Therefore, habitat segregation is excluded as
86 the underlying cause of these spatial segregations, and so they most likely reflect resource
87 competition. For LMP, segregation occurs between Charniid I and Ostrich Feather ($PCF_{Min}=0.$
88 4932 ; $p=0.01$; Figure 2d), and between Charniid II and Ostrich Feather ($PCF_{Min}=0.5346$;
89 $p=0.01$; Figure 2c). The large specimens of Charniid II and Ostrich Feather were segregated
90 ($p=0.01$), while small specimens were aggregated ($p=0.92$) thus resource competition is the most
91 likely underlying process. However, the Charniid I – Ostrich Feather bivariate distribution was
92 segregated across all size classes ($p_{small}=0.02$ and $p_{large}=0.01$; Supplementary Table 3), thus
93 likely reflecting habitat segregation rather than competition.

94 If resource competition dominates community dynamics and leads to tiering, then the
95 extent of DVS^{height} and/or $DVS^{uptake-zone}$ should predict whether two taxa exhibit inter-specific
96 competition, with high DVS taxon pairs not competing (as they occupy different parts of the
97 water column). This resource competition-dominated community dynamic is consistent with the
98 ‘D’ surface community, which exhibited high DVS , and had no instances of inter-specific
99 resource competition (Figs. 2, 3; Supplementary Table 3). However, on the ‘E’ surface, the two
100 instances of resource competition correspond to high levels of pairwise DVS^{uptake} with respect to
101 both Feather Dusters – *Fractofusus* and Feather Dusters – *Charniodiscus* (DVS^{uptake}_{FeaD-}

102 $Fract=75.1\%$; $DVS^{uptake}_{FeaD-Chard}=60.3\%$; Supplementary Table 3). On the ‘E’ surface, Charniids
103 and *Thectardis* both exhibit very low DVS^{uptake} levels ($DVS^{uptake}_{Charniid}=10.4\%$ and DVS^{uptake}_{Thect}
104 $=12.0\%$), but do not correspond to any of the instances of inter-specific competition
105 identified; neither do the comparatively high levels of uptake-zone tiering correspond to the
106 presence of resource competition (Figs. 2 and 3, Supplementary Table 1). The single LMP
107 instance of resource competition, between Charniid II and Ostrich Feather, corresponded to a
108 moderate level of pairwise DVS^{uptake} (38.8%), coupled to a very strong segregation
109 ($PCF_{Min}=0.4932$). A linear regression of the DVS^{uptake} with PCF_{Min} showed no significant
110 relationship ($p=0.283$), so our results from the ‘E’ and LMP surface provide no evidence that
111 resource competition resulted in vertically tiered populations.

112 When the E’ surface taxa were subset into rangeomorphs/non-rangeomorphs, and
113 stemmed/non-stemmed groups there were no significant differences in DVS^{uptake} or DVS^{height}
114 between rangeomorphs and non-rangeomorphs or stemmed and non-stemmed DVS^{uptake}
115 (Supplementary Table 2 ; all $p \gg 0.1$). There was a significant difference in DVS^{height} between
116 stemmed ($DVS^{height}_{stem}=4.0\%$) and non-stemmed taxa ($DVS^{height}_{non-stem}=19.9\%$; $p=0.001$).

117 The development of stems has been hypothesized to enable organism uptake-zone to
118 reach new water column heights, thus avoiding competition for resources^{7-9, 28} such as oxygen, or
119 the dissolved organic carbon which Mistaken Point organisms likely utilised^{28,29} (see Ref [2] for
120 further discussion). This hypothesis predicts that stemmed organisms should be more tiered (i.e.
121 higher DVS) than non-stemmed organisms, but our results disagree: non-stemmed taxa exhibit a
122 significantly higher degree of DVS^{height} than stemmed taxa (Supplementary Table 3). Thus, naked
123 stems likely had a different function, such as enabling greater offspring dispersal⁷. For dispersal-
124 generated aggregations, cluster size (Supplementary Tables 4-5) was found to strongly correlate

125 with maximum height of ‘E’ surface organisms ($R^2=0.997$, $p=0.034$), but not with mean height
126 or mean uptake-zone height (all $p \gg 0.1$). This result demonstrates that maximum height
127 directly resulted in greater offspring dispersal. Therefore, while stemmed organisms did not
128 significantly benefit from the additional height for nutrient acquisition, they did gain increased
129 offspring dispersal. While at least some Ediacaran species exhibited close-to-parent offspring
130 dispersal due to non-waterborne, stolon dominated reproduction¹¹, evidence of wide-spread
131 dispersal³⁰⁻³⁴ demonstrates the prevalence of Ediacaran waterborne propagation, and so the
132 importance of colonization potential for Ediacaran macrofossils.

133 The lack of correlation between *DVS* and resource competition throughout Mistaken
134 Point communities contradicts previous suggestions that competition for resources drove
135 Ediacaran community ecology^{2-4,6,28}. While increased height would have placed organisms in
136 faster water flow⁸, increasing resource refresh rates, the lack of tiering within these communities
137 demonstrates that these advantages were not significant. Additionally, we have shown that the
138 advantage of height in these communities was a larger radius of offspring clusters – representing
139 increased dispersal distances. Therefore, our results point to reproduction, not limited resources,
140 as the principal driver of the dynamics of these oldest complex macro-communities.

141 **Methods**

142 **Data.** We used the data compiled by Clapham et al. (2003)^{11,35} from the Lower Mistaken Point
143 (LMP), ‘D’ surface and ‘E’ surface which recorded the spatial position, size measurements and
144 orientation of each fossil. Specimens were recorded as one of fourteen taxonomic groups of
145 macrofossils, including two ‘bin’ groups³⁶: 1) *Bradgatia*, 2) *Pectinifrons*, 3) *Thectardis*, 4)
146 *Fractofusus andersoni* + *F. misrai*, 5) *Charniodiscus spinosus* + *C. procerus*, 6) “Feather
147 Dusters” which includes *Plumeropriscum* and *Primocandlebrum*, 7) *Hiemalora*, 8)

148 Ivesheadiomorphs³⁷, 9) Lobate Discs, which are interpreted either as taphomorphs
149 (dead/decaying remains) or as microbial colonies^{2,10,17}, 10) *Charnia* ‘A’ which consists of
150 *Beothukis mistakensis*^{38,39} (which dominates the ‘E’ surface) and *Charnia masoni*. 11) *Charnia*
151 ‘B’ now reassigned as *Trepassia wardae*³⁹. Charniid populations on Mistaken Point are
152 dominated by *Beothukis* (only four individuals on the ‘E’ surface are true *Charnia* species),
153 therefore direct comparison of data from this grouping with those from other taxonomic groups
154 should be undertaken with caution. 12) “Ostrich Feathers” 13) “Holdfast Discs”, being all
155 discoidal specimens of uncertain affinity, with or without associated stems, which lack sufficient
156 detail to identify the taxon, 14) “Other Species” being rare forms that do not fall into any of the
157 other groups; e.g., *Hapsidophyllas*.

158 **Methods.** Differential erosion has the potential to distort spatial analyses⁴⁰ so this data has been
159 tested for impact of differential erosion using heterogeneous Poisson models to model possible
160 sources of erosion¹¹, with no significant effects found on ‘D’ and ‘E’ surfaces. In this study we
161 fit three heterogeneous Poisson models to the LMP data, with the models dependent on x is
162 North to South (parallel to strike), y is East to West (parallel to dip), xy is the distance from the
163 South - East corner finding no significant erosional effect (all $p < 0.01$, where $p = 1$ corresponds to
164 a perfect model fit – the spatial distributions depend exactly on the covariant). The tectonically
165 distorted data was retrodeformed by returning elongated holdfast discs to a circular outline^{6,18}.

166 **Tiering metric.** We defined two different metrics for quantifying tiering: height Distinct
167 Vertical Stratification (DVS^{height}) and uptake-zone DVS^{uptake} . DVS^{height} is calculated by 1)
168 creating a frequency table in 1cm bins of the height of each specimen within that taxon
169 population. 2) A similar frequency table is created using the rest of the community. 3) The two
170 frequency tables are subtracted from each other and then 4) DVS^{height} for each taxon is calculated

171 as the percentage of specimens remaining divided by the total number of specimens of that
172 taxon. Community DVS^{height} is the mean of all the taxa DVS^{height} . DVS^{uptake} is calculated
173 similarly, but the frequency tables are created by filling in every 1cm that the specimen uptake-
174 zone occupies. For example, a 4cm *Bradgatia* would be represented by a count in the 0cm –
175 4cm bin, whereas a 4cm *Charniodiscus* with a 1cm stem would be represented by a count in the
176 1cm – 4cm bin. For example, $DVS=0\%$ corresponds to no taxa occupying a unique part of the
177 water column, i.e. the height distribution of that population is totally overlapped by the
178 populations of other taxa. $DVS=100\%$ corresponds to each taxon occupying a distinct stratum of
179 the water column, i.e. there is no overlap between specimens of any taxa.

180 Alternative metrics, such as overlap of a range (such as the interquartile range, or 95%
181 standard deviations) were ruled out because such range comparisons 1) assume a distribution e.g.
182 normal or log-normal, which isn't necessarily accurate; 2) outliers (such the giant *Fronndophyllas*
183 found on Lower Mistaken Point) severely bias the data and 3) such range metrics do not take
184 into account relatively frequency – many populations had relatively few specimens at the end of
185 their height range biasing the analyses.

186 Specimen heights were defined as the specimen length for *Bradgatia*, Charniid I,
187 *Thectardis*; specimen width for *Pectinifrons*; stem length plus frond length for Charniid II,
188 Feather Dusters, *Charniodiscus* and Ostrich Feathers. *Fractofusus* height was calculated a
189 quarter of its width, thus assuming the *Fractofusus* has two vanes. It has been suggested that
190 *Fractofusus* had three vanes⁴¹ which would increase its vertical height. Repeating our analyses
191 with height assuming three vanes reduces overall DVS^{height}_D by 9.3% to 70.8%, by 1.9% to
192 $DVS^{height}_E=10.9\%$ and by 4.9% to $DVS^{uptake}_E=40.0\%$, so did not significantly change our results.
193 Comparisons between DVS on the 'D', 'E' and LMP surfaces, and between the 'E' surface

194 community rangeomorphs/non-rangeomorphs and the stemmed/non-stemmed, were performed
195 using Mann-Whitney tests. To account for the non-independence of the shared-sites in the
196 pairwise comparisons of *DVS* on the ‘D’, ‘E’ and LMP surfaces, the significance level was set α
197 = $0.05/3 = 0.017$, but note that such adjustment is likely to be too conservative.

198 **Data availability.** Access to the fossil localities is by scientific research permit only. Natural
199 Areas Program, Canada for further information. Data used is publicly available at
200 https://figshare.com/articles/Mistaken_Point_Ediacaran_count_data/1111665

201 **Code availability.** The code defining these tiering metrics has been uploaded as an R package
202 (tiering) to <https://cran.r-project.org/>.

203 **Spatial analyses.** Initial data exploration, inhomogeneous Poisson modelling, residual analysis
204 and segregation tests²³ were performed in R⁴² using the package spatstat⁴³⁻⁴⁵. Programita⁴⁶⁻⁵⁰ was
205 used to find distance measures and to perform aggregation model fitting (described in detail in
206 references^{44,46-50}).

207 Bivariate PCFs were calculated from the population density using a grid of 10cm x 10cm
208 cells on the ‘D’ and ‘E’ surfaces, and 1cm x 1cm on LMP. To minimize noise a smoothing was
209 applied to the PCF dependent on specimen abundance: A three cell smoothing over this grid was
210 applied to the ‘D’ and ‘E’ surfaces, with five cells for LMP.

211 To test whether the PCF exhibited complete spatial randomness (CSR), 999 simulations
212 were run for each relationship on a homogeneous background to generate simulation envelopes
213 around the completely spatially random (CSR) which is where the PCF=. The fit of the fossil
214 data to CSR was tested using Diggle’s goodness-of-fit test²² p_d (where $p_d=1$ corresponds to CSR,
215 and $p_d=0$ corresponds to non-CSR) with PCF deviations outside the simulation envelope coupled
216 to a $p_d \ll 1$ taken to indicate significantly non-CSR distributions. Note that due to non-

217 independence of spatial data, Monte-Carlo generated simulation envelopes cannot be interpreted
218 as confidence intervals⁴⁷, and also run the risk of Type I errors if the observed PCF falls near the
219 edge of the simulation envelope²¹ so that hypothesis testing needs to be further supplemented.
220 None-the-less, if the observed data fell below the Monte-Carlo simulations, the bivariate
221 distribution was described as segregated, and above the Monte-Carlo simulations the bivariate
222 distribution was described as aggregated. Non-CSR distributions were tested for statistical
223 significance using Diggle's goodness-of-fit test²², with segregations further tested using Diggle's
224 segregation test²³ (Supplementary Table 3). Diggle's goodness-of-fit test, is a single test
225 statistic²¹ (p_d) representing the total squared deviation between the observed pattern and the
226 theoretical result across the studied distances. This test statistic was used in conjunction with
227 visual inspection of Monte Carlo simulations for two reasons. First, p_d does not strictly test
228 whether a model should be accepted or rejected, but whether the PCFs for the observed data are
229 within the range of the stochastic realization of the model²⁶. Second, p_d depends on the range
230 over which it is calculated. Diggle's segregation test²³, detects where two types (taxa here) are
231 spatially segregated by calculating the sum of the square of the probability that each data point is a
232 given type (taxa) minus the average fraction of data points which are a given type (taxa).

233 If a taxon was not randomly distributed on a homogeneous background, and was aggregated
234 (Figure 2, Supplementary Table 4), the random model on a heterogeneous background was tested
235 by creating a heterogeneous background from the density map of the taxon under consideration,
236 being defined by a circle of radius R over which the density is averaged throughout the sample
237 area. Density maps were formed using estimators within the range of $0.1m < R < 1m$, and the R
238 corresponding to the best-fit model was used. If excursions outside the simulation envelopes for

239 both homogeneous and heterogeneous Poisson models remained, then Thomas cluster models
240 were fitted to the data as follows:

241

242 1. The PCF and L function⁵¹ of the observed data were found. Both measures were
243 calculated to ensure that the best-fit model is not optimized towards only one distance measure,
244 and thus encapsulates all spatial characteristics.

245 2. Best-fit Thomas cluster processes⁵² were fitted to the two functions where $PCF > 1$. The
246 best-fit lines were not fitted to fluctuations around the random line of $PCF = 1$ in order to aid good
247 fit about the actual aggregations, and to limit fitting of the model about random fluctuations.
248 Programita used the minimal contrast method²¹⁻²³ to find the best-fit model.

249 3. If the model did not describe the observed data well, the lines were refitted using just the
250 PCF. If that fit was also poor, then only the L-function was used.

251 4. 99 simulations of this model were generated to create simulation envelopes, and the fit
252 checked using the O-ring statistic⁴⁶.

253 5. p_d was calculated over the model range. Very small-scale segregations (under 2cm) were
254 not included in the model fitting, since they likely represent the finite size of the specimens, and
255 the lack of specimen overlap.

256 6. If there were no excursions outside the simulation envelope and the p_d -value was high,
257 then a univariate homogeneous Thomas cluster model was interpreted as the best model.

258 The most objective way to resolve the number and range of size classes in a population is
259 by fitting height-frequency distribution data to various models, followed by comparison of
260 (logarithmically scaled) Bayesian information criterion (BIC) values⁵⁵, which we performed in R
261 using the package MCLUST⁵⁶. The number of populations thus identified was then used to

262 define the most appropriate size classes. A BIC value difference of > 10 corresponds to a
263 “decisive” rejection of the hypothesis that two models are the same, whereas values < 6 indicate
264 only weakly reject similarity of the models⁵⁵⁻⁵⁷.

265 Once defined, the PCFs for each size class were calculated, and segregated tests performed.
266 Although it was necessary to set firm boundaries for each size class, the populations are normally
267 distributed and therefore overlap. As a result, the largest individuals of the small population are
268 grouped within the middle size class, while some of the smallest of the medium population are
269 included within the small size class. As such, the medium population was excluded from
270 analyses.

271 For each bivariate distribution displaying segregation, the size-classes of each taxon were
272 calculated, the bivariate PCFs of the smallest size-classes and largest size-classes were plotted
273 with 99 Monte Carlo simulations of a complete spatially random distribution and segregation
274 tests performed.

275 **Regression analyses.** In order to investigate the relationship between height and dispersal linear
276 regressions were performed in R⁴¹. Programita⁴⁶⁻⁵⁰ was used to find the taxa whose univariate
277 distributions were best modelled by Thomas Cluster models (thus most likely to be dispersal
278 induced) and the best-fit cluster radius was used to indicate dispersal range. Four different
279 height variables were found for each taxon’s population 1) Mean height 2) Maximum height, 3)
280 Mean mid-point of uptake-zone and 4) Maximum mid-point of uptake zone. The uptake-zone
281 mid-point for each specimen was calculated as the half-way point between the top of the stem
282 and the top of the frond and was a proxy for dispersal release throughout the entire uptake-zone.

283
284
285
286
287
288
289
290
291
292
293
294
295
296
297
298
299
300
301
302
303
304

References

1. Pu, J.P., Bowring, S.A., Ramezani, J., Myrow, P., Raub, T.D., Landing, E., Mills, A., Hodgkin, E. and Macdonald, F.A.. Dodging snowballs: Geochronology of the Gaskiers glaciation and the first appearance of the Ediacaran biota. *Geology*, **44**, 955-958 (2016).
2. Liu, A. G, Kenchington C. G. & Mitchell, E. G. Remarkable insights into the paleoecology of the Avalonian Ediacaran biota. *Gondwana Res.* **27**, 1355–1380 (2015).
3. Butterfield, N. J. Animals and the invention of the Phanerozoic Earth system. *Trends in Ecology & Evolution* **26**, 81-87 (2011).
4. Woodward, G., Ebenman, B., Emmerson, M., Montoya, J.M., Olesen, J.M., Valido, A. and Warren, P.H.. Body size in ecological networks. *Trends in ecology & evolution*, **20**, 402-409 (2005).
5. Liu, A. G., McIlroy, D., & Brasier, M. D. First evidence for locomotion in the Ediacara biota from the 565 Ma Mistaken Point Formation, Newfoundland. *Geology*, **38**, 123-126 (2010).
6. Clapham, M. E., & Narbonne G. M., Gehling, J. G. Ediacaran epifaunal tiering. *Geology*, **30**, 627-630 (2002).
7. Laflamme, M., Flude, L. I., & Narbonne, G. M. Ecological tiering and the evolution of a stem: the oldest stemmed frond from the Ediacaran of Newfoundland, Canada. *Journal of Palaeontology*, **86**, 193-200 (2012).
8. Ghisalberti, M., et al.. Canopy flow analysis reveals the advantage of size in the oldest communities of multicellular eukaryotes. *Current Biology*, **24** 305-309 (2014).
9. Laflamme, M., & Narbonne, G. M.. Ediacaran fronds. *Palaeogeography, Palaeoclimatology, Palaeoecology*, **258**, 162-179 (2008).

- 305 10. Mitchell, E. G & Butterfield, N. J. Spatial analyses of Ediacaran communities at Mistaken
306 Point. *Paleobiology*, **44**, 40-57. (2018).
- 307 11. Mitchell, E. G., Kenchington, C. G., Liu, A. G., Matthews, J. J., & Butterfield, N. J.
308 Reconstructing the reproductive mode of an Ediacaran macro-organism. *Nature*, **524**, 343-
309 346 (2015).
- 310 12. Clapham, M. E., Narbonne, G.M. & Gehling, J. G. Paleocology of the oldest known animal
311 communities: Ediacaran assemblages at Mistaken Point, Newfoundland. *Paleobiology* **29**,
312 527–544 (2003).
- 313 13. Landing, E., Narbonne, G.M. & Myrow, P. (eds) Trace fossils, small shelly fossils and the
314 Precambrian–Cambrian boundary. *Bull. NY State Mus.* **463**, 1–81 (1988).
- 315 14. Narbonne, G. M. Modular construction of early Ediacaran complex life forms. *Science* **305**,
316 1141–1144 (2004).
- 317 15. Hoyal Cuthill, J. F. & Conway Morris, S. Fractal branching organizations of Ediacaran
318 rangeomorph fronds reveal a lost Proterozoic body plan. *Proc. Natl Acad. Sci. USA* **111**,
319 13122–13126 (2014).
- 320 16. Brasier, M. D., Antcliffe, J. B. & Liu, A. G. The architecture of Ediacaran fronds.
321 *Palaeontology* **55**, 1105–1124 (2012).
- 322 17. Liu, A. G., McIlroy, D., Antcliffe, J. B. & Brasier, M. D. Effaced preservation in the
323 Ediacara biota and its implications for the early microfossil record. *Palaeontology* **54**, 607–
324 630 (2011).
- 325 18. Wood, D. A., Dalrymple, R. W., Narbonne, G. M., Gehling, J. G. & Clapham, M. E.
326 Paleoenvironmental analysis of the late Neoproterozoic Mistaken Point and Trepassey
327 formations, southeastern Newfoundland. *Can. J. Earth Sci.* **40**, 1375–1391 (2003).

- 328 19. Benus, A. P. Sedimentological context of a deep-water Ediacaran fauna (Mistaken Point
329 Formation, Avalon zone, eastern Newfoundland). *Bull. NY State Mus.* **463**, 8–9 (1988).
- 330 20. Illian, J., Penttinen, A., Stoyan, H. & Stoyan, D. *Statistical Analysis and Modelling of*
331 *Spatial Point Patterns* Vol. 70 (John Wiley, 2008).
- 332 21. Diggle, P. *Statistical Analysis of Spatial Point Patterns* 2nd edn (Arnold, 2003).
- 333 22. Diggle, P., Zheng, P. and Durr, P.. Nonparametric estimation of spatial segregation in a
334 multivariate point process: bovine tuberculosis in Cornwall, UK. *Journal of the Royal*
335 *Statistical Society: Series C (Applied Statistics)*, **54**, 645-658 (2005).
- 336 23. Wiegand, T., Gunatilleke, S., Gunatilleke, N. & Okuda, T. Analyzing the spatial structure of
337 a Sri Lankan tree species with multiple scales of clustering. *Ecology* **88**, 3088–3102 (2007).
- 338 24. Levin, S. A. in *Ecological Time Series Vol.2* (eds Powell, T. M. & Steele, J. H.) 277–326
339 (Springer, 1995).
- 340 25. McIntire, E. J. & Fajardo, A. Beyond description: the active and effective way to infer
341 processes from spatial patterns. *Ecology* **90**, 46–56 (2009).
- 342 26. Wiegand, T. & Moloney, K. A. *Handbook of Spatial Point-Pattern Analysis in Ecology*
343 (CRC, 2013).
- 344 27. Murrell, D.J. and Law, R.. Heteromyopia and the spatial coexistence of similar
345 competitors. *Ecology letters*, **6**,48-59 (2003).
- 346 28. Hoyal Cuthill, J.F. and Conway Morris, S. Nutrient-dependent growth underpinned the
347 Ediacaran transition to large body size. *Nature ecology & evolution*, **1**,1201 (2017).
- 348 29. Laflamme, M., Xiao, S., & Kowalewski, M. Osmotrophy in modular Ediacara organisms.
349 *Proc. Natl Acad. Sci. USA*, **106**, 14438-14443 (2009).

- 350 30. Darroch, S. A. F., Laflamme, M. & Clapham, M. E. Population structure of the oldest known
351 macroscopic communities from Mistaken Point, Newfoundland. *Paleobiology* **39**, 591–608
352 (2013).
- 353 31. Droser, M. L. & Gehling, J. G. Synchronous aggregate growth in an abundant new Ediacaran
354 tubular organism. *Science* **319**, 1660–1662 (2008).
- 355 32. Penny, A. M. et al. Ediacaran metazoan reefs from the Nama Group, Namibia. *Science* **344**,
356 1504–1506 (2014).
- 357 33. Yuan, X. et al. The Lantian biota: a new window onto the origin and early evolution of
358 multicellular organisms. *Chin. Sci. Bull.* **58**, 701–707 (2013).
- 359 34. Hua, H., Chen, Z., Yuan, X., Zhang, L. & Xiao, S. Skeletogenesis and asexual reproduction
360 in the earliest biomineralizing animal Cloudina. *Geology* **33**, 277–280 (2005).
- 361 35. Clapham, M. E. Ordination methods and the evaluation of Ediacaran communities.
362 In: *Quantifying the Evolution of Early Life* (pp. 3–21). Ed. Laflamme, Marc, Schiffbauer,
363 James D., Dornbos, Stephen Q. Springer Netherlands (2011).
- 364 36. Shen, B., Dong, L., Xiao, S. & Kowalewski, M. The Avalon explosion: evolution of
365 Ediacara morphospace. *Science* **319**, 81–84 (2008)
- 366 37. Liu, A. G., McIlroy, D., Antcliffe, J. B. & Brasier, M. D. Effaced preservation in the
367 Ediacara biota and its implications for the early macrofossil record. *Palaeontology* **54**, 607–
368 630 (2011)
- 369 38. Narbonne, G. M., Laflamme, M., Greentree, C. & Trusler, P. Reconstructing a lost world:
370 Ediacaran rangeomorphs from Spaniard's Bay, Newfoundland. *J. of Paleontology* **83**, 503–
371 523 (2009)

- 372 39. Brasier, M. D. & Antcliffe, J. B. Evolutionary relationships within the Avalonian Ediacara
373 biota: new insights from laser analysis. *Journal of the Geological Society* **166**, 363-384
374 (2009).
- 375 40. Matthews, J.J., Liu, A.G. and McIlroy, D.. Post-fossilization processes and their
376 implications for understanding Ediacaran macrofossil assemblages. *Geological Society,*
377 *London, Special Publications*, **448**, 251-269 (2017).
- 378 41. Narbonne, G.M., Laflamme, M., Trusler, P.W., Dalrymple, R.W. and Greentree, C.. Deep-
379 water Ediacaran fossils from northwestern Canada: taphonomy, ecology, and
380 evolution. *Journal of Paleontology*, **88**, 207-223 (2014).
- 381 42. R Core Team. *R: A Language and Environment for Statistical Computing*. R Foundation for
382 Statistical Computing Vienna, Austria (2013)
- 383 43. Baddeley, A. & Turner, R. Spatstat: an R package for analyzing spatial point patterns. *J. of*
384 *Statistical Software* **12**, 1–42 (2005)
- 385 44. Berman, M. Testing for spatial association between a point process and another stochastic
386 process. *Applied Statistics* **35**, 54–62 (1986)
- 387 45. Baddeley, A., Rubak, E. & Møller, J. Score, pseudo-score and residual diagnostics for
388 spatial point process models. *Statistical Science* **26**, 613–646 (2011)
- 389 46. Wiegand, T. & Moloney, K. Rings, circles, and null-models for point pattern analysis in
390 ecology. *Oikos* **104**, 209–229 (2004)
- 391 47. Wiegand, T., Kissling, W., Cipriotti, P. & Aguiar, M. Extending point pattern analysis for
392 objects of finite size and irregular shape. *J. of Ecology* **94**, 825–837 (2006)

- 393 48. Wiegand, T., Moloney, K., Naves, J. & Knauer, F. Finding the missing link between
394 landscape structure and population dynamics: a spatially explicit perspective. *The American*
395 *Naturalist* **154**, 605–627 (1999)
- 396 49. Loosmore, N. B. & Ford, E. D. Statistical inference using the G or K point pattern spatial
397 statistics. *Ecology* **87**, 1925–1931 (2006)
- 398 50. Wiegand, T. & Moloney, K. A. *Handbook of Spatial Point-pattern Analysis in Ecology*. 538
399 pages. CRC Press (2013)
- 400 51. Levin, S. A. *The problem of pattern and scale in ecology* (pp. 277–326). Springer U.S.
401 (1995)
- 402 52. Besag, J. Spatial interaction and the statistical analysis of lattice systems. *J. of the Royal*
403 *Statistical Society. Series B (Methodological)* **36**, 192–236 (1974)
- 404 53. Thomas, M. A generalization of Poisson’s binomial limit for use in ecology. *Biometrika* **36**,
405 18–25 (1949)
- 406 54. Grabarnik, P., Myllymäki, M. & Stoyan, D. Correct testing of mark independence for
407 marked point patterns. *Ecological Modelling* **222**, 3888–3894 (2011)
- 408 55. Fraley, C. & Raftery, A. E. *MCLUST version 3: an R package for normal mixture modeling*
409 *and model-based clustering*. Washington University Seattle Dept of Statistics (2006)
- 410 56. Fraley, C. & Raftery, A. E. Bayesian regularization for normal mixture estimation and
411 model-based clustering. *J. of Classification* **24**, 155–188 (2007)
- 412 57. Péliissier, R. & Goreaud, F. A practical approach to the study of spatial structure in simple
413 cases of heterogeneous vegetation. *J. of Vegetation Science* **12**, 99–108 (2001)
- 414 58. Stoyan, D., Kendall, W. S. & Mecke, J. *Stochastic geometry and its applications*. 2nd
415 edition. 458 pages. Springer Verlag (1995)

416

417 **Acknowledgments:** We thank N. Butterfield and A. Liu for discussions on this manuscript. The
418 Parks and Natural Areas Division, Department of Environment and Conservation, Government
419 of Newfoundland and Labrador provided permits to conduct research within the Mistaken Point
420 Ecological Reserve in 2010, 2016 and 2017. This work has been supported by the Natural
421 Environment Research Council [grant number NE/P002412/1], Gibbs Travelling Fellowship
422 from Newnham College, Cambridge and a Henslow Junior Research Fellowship from
423 Cambridge Philosophical Society to E. G. M.

424 **Author contributions.** E.G.M and C. G. K conceived the project, discussed the results and
425 prepared the manuscript. E. G. M. conceived and ran the analyses.

426

427 The authors declare no competing interests.

428

429

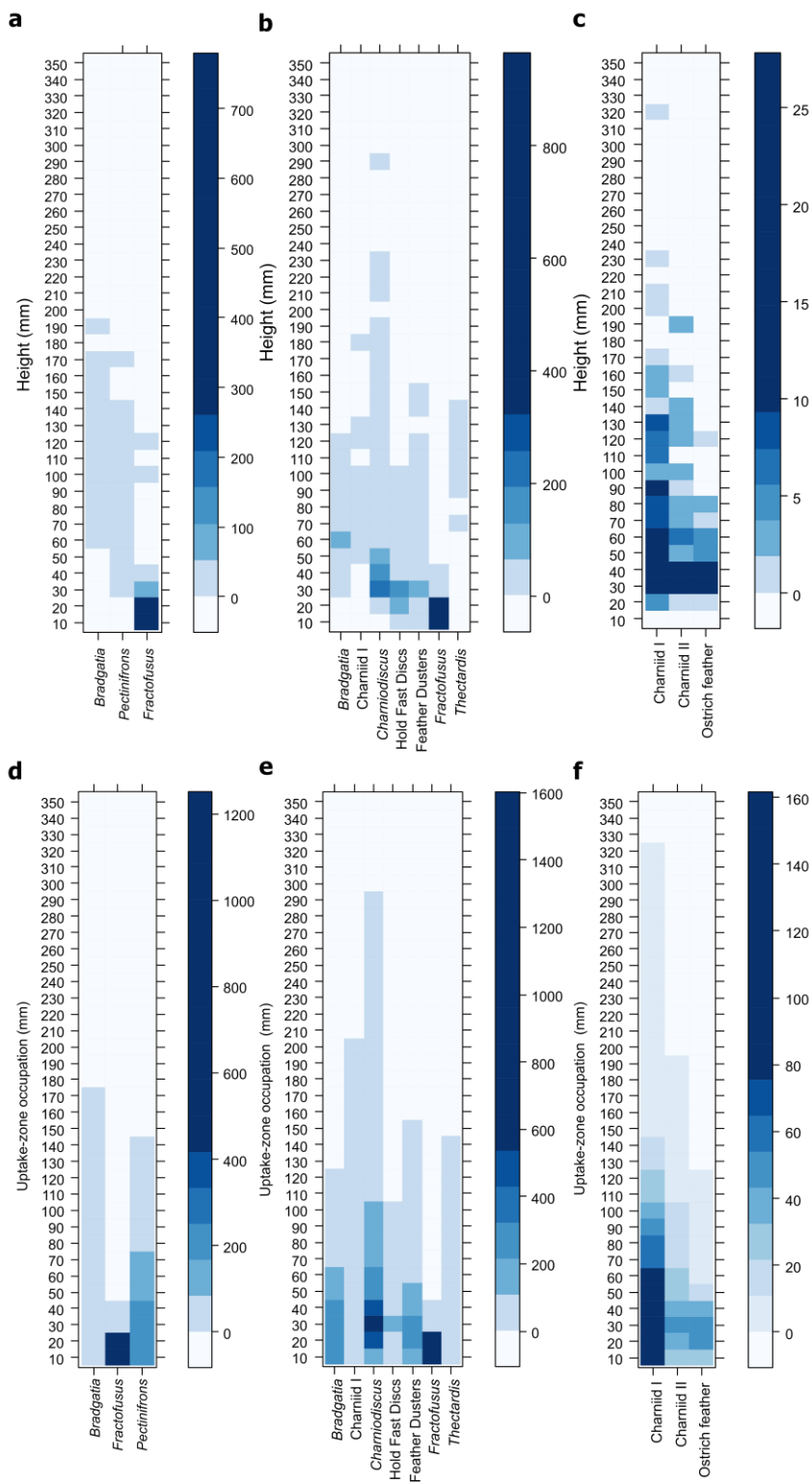
430

431

432

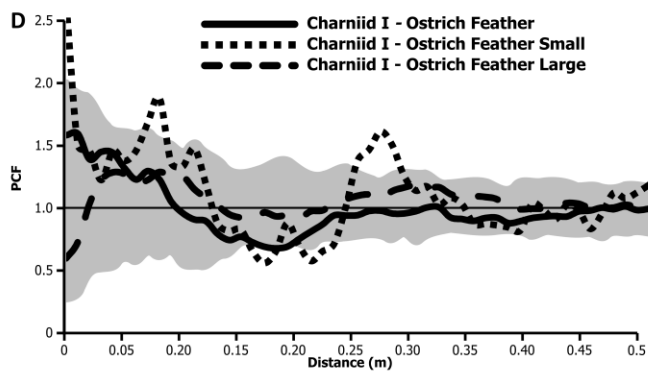
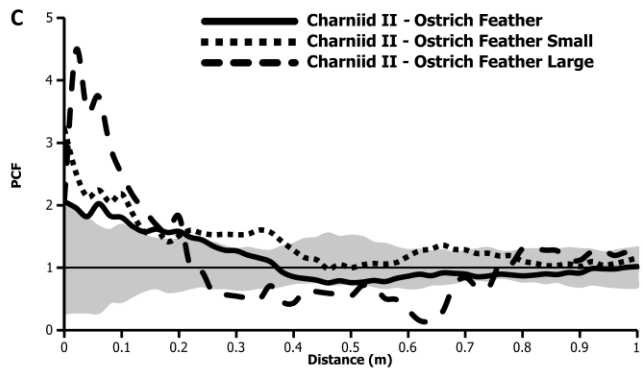
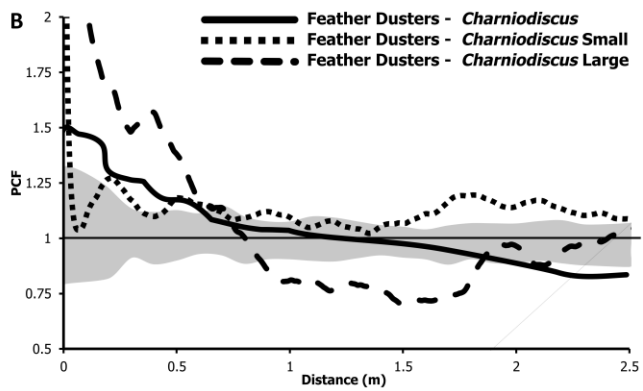
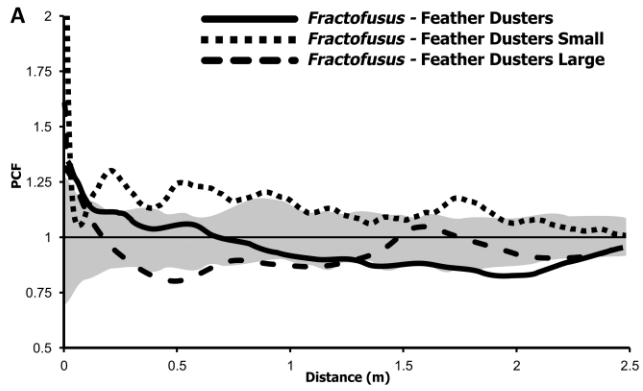
433

434



436 **Figure 1. DVS for Mistaken Point communities.** Height distributions of the **a**, ‘D’ surface
437 community **b**, ‘E’ surface community and the **c**, LMP surface community, and uptake-zone
438 distributions of the **d**, ‘D’ surface community **e**, ‘E’ surface community and the **f**, LMP
439 surface community. The taxonomic group is given on the *x*-axis, and the *y*-axis is the height
440 above the substrate in millimetres. The shade of the bin is given by the scale to the right of each
441 community plot, and represents the frequency of specimens at the given height (**a-c**) and the
442 occupation frequency of specimen uptake-zone (**d-f**). For example, in the height frequency plots
443 (**a-c**), a 56mm tall specimen with or without a stem would feature in the 50-60mm box only. For
444 the uptake-zone occupancy plots (**d-f**), a non-stemmed specimen 56mm tall would be shown in
445 the 10, 20, 30, 40, 50 and 60mm bins. A stemmed specimen 56mm tall with a 30mm stem would
446 be shown in the 40, 50 and 60mm bins.

447



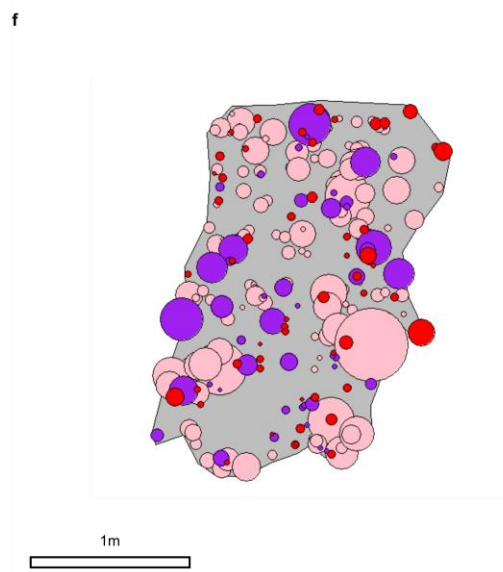
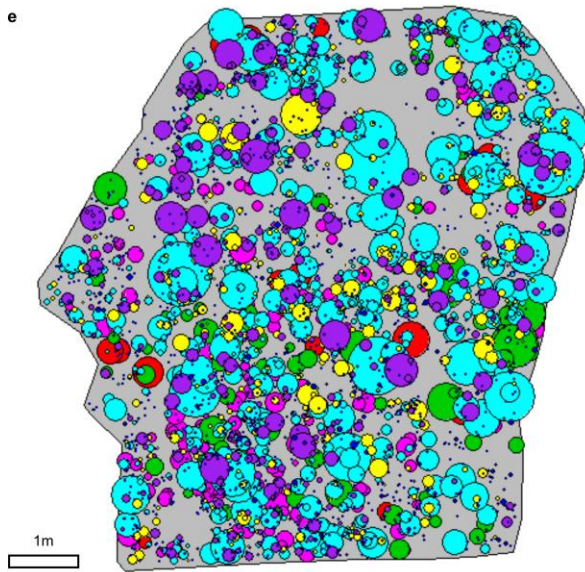
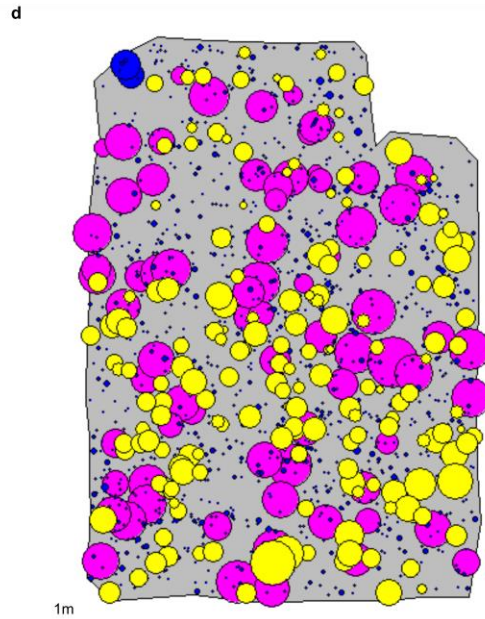
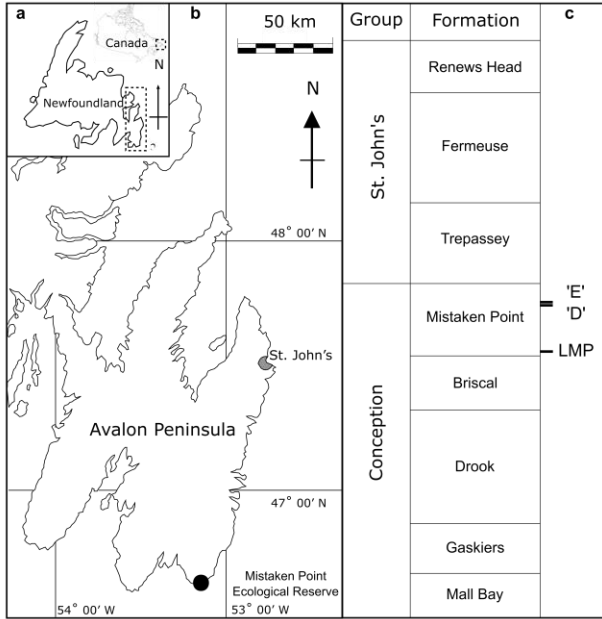
449 **Figure 2. PCF for resource competition interactions.** The x-axis is the inter-point distance
450 between organisms in meters. On the y-axis, PCF=1 indicates CSR, <1 indicates segregation and
451 >1 indicates aggregation. The grey shaded area denotes the boundaries of 99 Monte Carlo
452 simulations of CSR. Since the PCF curves are not within these areas, the complete spatial
453 randomness (CSR) hypotheses is rejected and one can assume that the distributions on both
454 surfaces are aggregated at small spatial scales and segregated at large spatial scales. ($p_d^{Fract-FeaD}$
455 < 0.01 , $p_d^{Chard-FeaD} < 0.01$, $p_d^{CharI-IOst} < 0.01$, $p_d^{CharII-IOst} < 0.01$). **a**, PCFs for ‘E’ surface
456 *Fractofusus* – Feather Dusters (1497 *Fractofusus* specimens of which 126 were small and 303
457 were large and Feather Dusters 362 specimens of which 296 were small and 66 large). **b**, PCFs
458 for ‘E’ surface *Charniodiscus* – Feather Dusters (*Charniodiscus* 825 specimens of which 489
459 were small and 336 were large and Feather Dusters 362 specimens of which 296 were small and
460 66 large). **c**, PCF for the segregated aggregation of the LMP surface (Charniid II 51 specimens of
461 which 26 were small and 25 were large and Ostrich Feather 54 specimens of which 38 were
462 small and 16 large). **d**, PCF for the segregated aggregation of the LMP surface (Charniid I 143
463 specimens of which 47 were small and 25 were large and Ostrich Feather 54 specimens of which
464 38 were small and 16 large).

465

466

467

468



470 **Supplementary Figure 1.**

471 **Map and simplified stratigraphic column showing the position of studied bedding planes**

472 **with bedding plane maps. a,** Newfoundland, eastern Canada. Dashed area indicates

473 region of interest in b. **b,** The Avalon Peninsula, eastern Newfoundland. Locations of the

474 bedding planes are indicated. **c,** Stratigraphic column (not to scale) of the Avalon Peninsulas.

475 The ‘E’ surface at Mistaken Point has been dated to $566 \pm 0.3\text{Ma}$ (ref. 1). **d-e,** Maps of the ‘D’,

476 ‘E’ and LMP surfaces showing specimen position and height (circle diameter). **d,** ‘D’ surface,

477 showing *Fractofusus* (blue), *Pectinifrons* (yellow) and *Bradgatia* (Pink). **e,** ‘E’ surface with

478 *Charniodiscus* (red), Holdfast discs with stems (orange), Charniid I (green), *Thectardis* (purple),

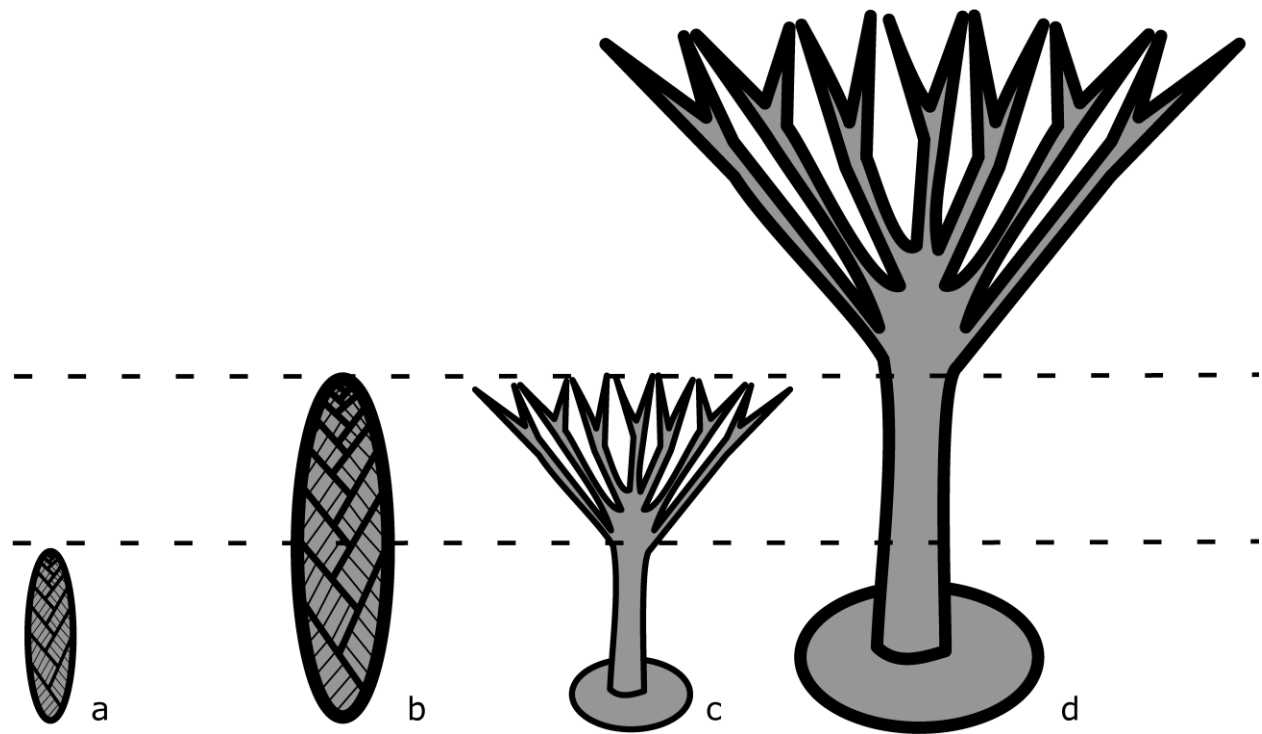
479 *Fractofusus* (blue), *Bradgatia* (pink) and Feather Dusters (yellow) and **f,** Lower Mistaken Point

480 showing Charniid A (I), Charniids II (purple) and Ostrich Feathers (red). Data from [12]. Scale

481 bar 1m.

482

483

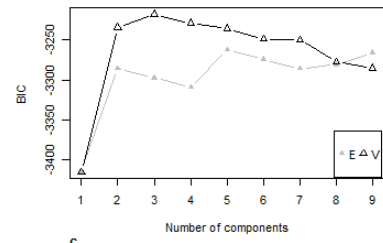
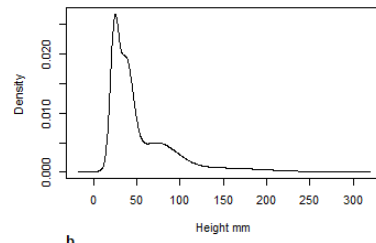
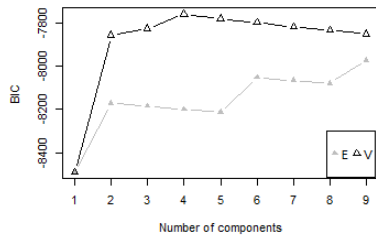


484

485 **Supplementary Figure 2. Diagram illustrating DVS and uptake-zone quantification.**

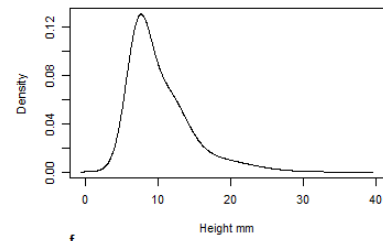
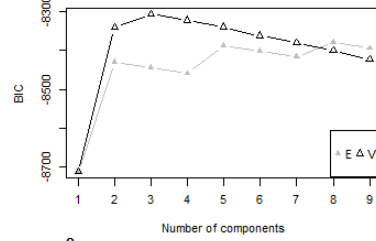
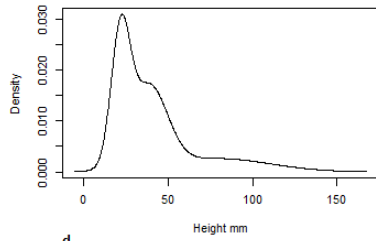
486 Uptake-zone was defined as the part of the organism which exhibited multiple scales of
 487 branching. In specimens i and ii, the uptake-zone consists of the entire height because they lack
 488 a naked stem. For specimens iii and iv, the uptake-zone is only the top 50% of the specimen, as
 489 the naked stem comprises the other 50%. To calculate *DVS*, the specimens within each taxon
 490 population were tabulated into 1cm height bins firstly using their height, and secondly their
 491 uptake-zone height ranges. For the above community (consisting of specimens i – iv), for the
 492 Charniid specimens (specimens i and ii), specimen i occupies a distinct stratum to the Feather
 493 Dusters (specimens iii and iv), while specimen ii height overlaps specimen iii in, and thus does
 494 not occupy a distinct stratum from Feather Dusters: consequently, the Charniids have a DVS^{height}
 495 = 50%. For the Feather Dusters (specimens iii and iv), specimen iii overlaps with ii, so does not
 496 occupy a distinct stratum, but specimen iv is not overlapped by any Charniid specimens: so,
 497 Feather Duster $DVS^{height} = 50\%$. Community DVS^{height} is the mean of the values for all taxa in the

498 community: $DVS^{height}_{Community} = 50\%$. The uptake-zone $DVS^{uptake}_{Community} = 50\%$ as well,
499 because the uptake-zones of specimens i and iv occupy distinct strata, but ii and iii do not.
500



b.

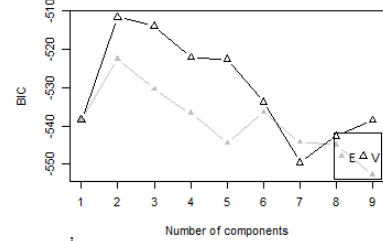
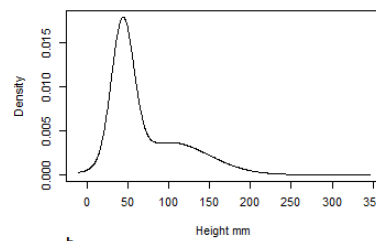
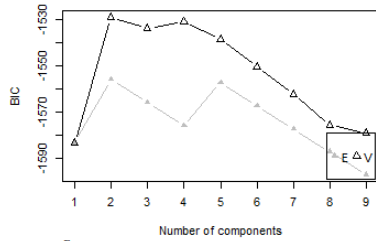
c.



d.

e.

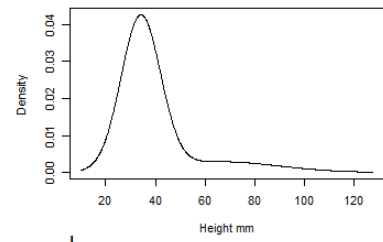
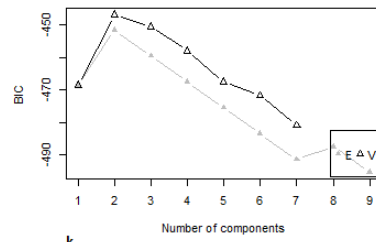
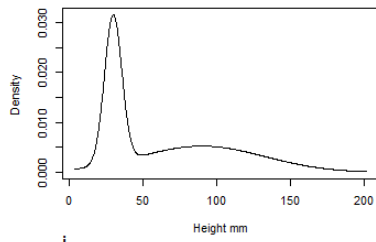
f.



g.

h.

i.



j.

k.

l.

504
505
506
507
508
509
510
511
512
513
514

Supplementary Figure 3.

Size distribution analysis of taxa with segregated bivariate PCFs. Size distribution analysis of taxa with segregated bivariate PCFs. **a**, ‘E’ surface *Charniodiscus* height-frequency distributions, and **b**, the results of Bayesian Information Criterion^{54,55} (BIC). Triangles and squares correspond to models assuming equal and unequal variance respectively. High BIC values correspond to a good model fit, so the best-fit model is a three component equal variance model. **c**, ‘E’ surface Feather Dusters height-frequency distributions and **d**, BIC. **e**, ‘E’ surface *Fractofusus* height-frequency distributions and **f**, BIC. **g**, LMP Charniid I height-frequency distributions, and **h**, BIC. **i** LMP Charniid II height-frequency distributions, and (J), BIC, (K), LMP Ostrich Feathers height-frequency distributions, and **j**, BIC.

Surface Taxon	Height DVS			Uptake-zone DVS		
	D	E	LMP	D	E	LMP
<i>Bradgatia</i>	0.6184	0.0000		0.6184	0.4204	
Charniid		0.0000	0.5232		0.1071	0.6821
Charniid II			0.0784			0.2549
<i>Charniodiscus</i>		0.0776			0.5806	
Feather Dusters		0.0000			0.0359	
<i>Fractofusus</i>	0.9957	0.7963		0.9957	0.8831	
Ostrich Feather			0.0000			0.2778
<i>Pectinifrons</i>	0.8057			0.8057		
<i>Thectardis</i>		0.0000			0.1200	

515 **Supplementary Table 1. Table of DVS values for Mistaken Point communities.** Table of
516 height and uptake-zone DVS for each taxon population within each of D, E and LMP
517 communities. *DVS* = 0% corresponds to no specimens occupying a unique part of the water
518 column, i.e. the height distribution of that population is totally overlapped by other taxa
519 populations. *DVS* =100% corresponds to no overlap between any specimens, so each taxon
520 occupies a distinct strata.

521

522

Surface	D	E	Lower Mistaken Point
Rangeomorph	96.96%	55.15%	71.82%
Stemmed	0.54%	30.18%	42.27%
Other	2.5%	14.67%	14.09%

523

Supplementary Table 2.

524

Community compositions. Percentage of taxa from each surface that are rangeomorphs and

525

have stemmed. The “Other category” refers to taxa which cannot be placed as either

526

Rangeomorphs or stemmed taxa due to lack of taxonomic certainty.

527

Surface	Taxon 1	Taxon 2	PCF _{min}	Size class <i>p</i> value	
				Small	Large
E	<i>Fractofusus</i>	Feather Dusters	0.8852	0.25	0.01
E	Feather Dusters	<i>Charniodiscus</i>	0.8972	0.14	0.01
LMP	Charniid I	Ostrich Feather	0.4932	0.02	0.01
LMP	Charniid II	Ostrich Feather	0.5346	0.92	0.01

528

529

Supplementary Table 3.

530

Segregation test for the different size-classes of segregated bivariate distributions. A value

531

of $p < 0.05$ is significantly segregated, while $p > 0.05$ is not significantly segregated.

532

Surface	Taxon	σ (m)	Mean Height (mm)	Maximum Height (mm)	Mean mid-point of Uptake-zone (mm)	Maximum mid-point of Uptake-zone (mm)
E	<i>Charnidiscus</i>	0.07	54	291	30	58
E	Feather Duster	0.25	41	153	43	106
E	<i>Thectardis</i>	0.18	102	165	16	104
LMP	Charniid II	0.22	63	185	26	93
LMP	Ostrich Feather	0.18	39	118	14	34

533

Supplementary Table 4.

534

Taxon height and cluster sizes. The best-fit cluster size for the Thomas Cluster model of each

535

frondose taxon exhibiting Thomas Cluster aggregation^{4,5}. The mid-point of the active zone

536

height is given by calculating the mid-point between the stem and the top of the frond for each

537

specimen.

538

Surface	Top of Stem Height				Uptake-zone height				Top of frond Height			
	Mean		Max		Mean		Max		Mean		Max	
	<i>p</i>	R ²	<i>p</i>	R ²	<i>p</i>	R ²	<i>p</i>	R ²	<i>p</i>	R ²	<i>p</i>	R ²
E	<i>0.47</i>	0.54	<i>0.48</i>	0.54	<i>0.78</i>	0.12	<i>0.28</i>	0.82	<i>0.88</i>	0.04	<i>0.03</i>	1.00

539

540

Supplementary Table 5.

541

Linear regression analyses. Linear regressions of the fitted cluster sizes of Table S3 for

542

frondose organisms showing a Thomas Cluster i.e. dispersal process aggregations. The

543

regressions which are significant are given in bold. These analyses could not be repeated for

544

LMP surface due to insufficient sample size.

545

546

547